Data in Brief 17 (2018) 837–841

Contents lists available at ScienceDirect

Data in Brief

journal homepage: www.elsevier.com/locate/dib

Data article

Data and videos for ultrafast synchrotron X-ray imaging studies of metal solidification under ultrasound

Bing Wang [a,b], Dongyue Tan [a], Tung Lik Lee [a,c], Jia Chuan Khong [a,d], Feng Wang [e], Dmitry Eskin [e], Thomas Connolley [f], Kamel Fezzaa [g], Jiawei Mi [a,*]

[a] School of Engineering & Computer Science, University of Hull, Hull, HU6 7RX, UK
[b] Department of Engineering, University of Cambridge, CB2 1PZ, UK
[c] ISIS Neutron Source, Rutherford Appleton Laboratory, Harwell Oxford, Didcot, OX11 0QX, UK
[d] Department of Medical Physics and Biomedical Engineering, University College London, London WC1E 6BT, UK
[e] Brunel Centre for Advanced Solidification Technology, Brunel University London, Uxbridge, London, UB8 3PH, UK
[f] Diamond Light Source Ltd., Harwell Science & Innovation Campus, Didcot, OX11 0DE, UK
[g] Advanced Photon Source, Argonne National Laboratory, Argonne, IL 60439, USA

ARTICLE INFO

Article history:
Received 2 November 2017
Accepted 30 January 2018
Available online 8 February 2018

ABSTRACT

The data presented in this article are related to the paper entitled 'Ultrafast synchrotron X-ray imaging studies of microstructure fragmentation in solidification under ultrasound' [Wang et al., Acta Mater. 144 (2018) 505-515]. This data article provides further supporting information and analytical methods, including the data from both experimental and numerical simulation, as well as the Matlab code for processing the X-ray images. Six videos constructed from the processed synchrotron X-ray images are also provided.

DOI of original article: https://doi.org/10.1016/j.actamat.2017.10.067
* Corresponding author.
E-mail address: j.mi@hull.ac.uk (J. Mi).

https://doi.org/10.1016/j.dib.2018.01.110

Specifications Table

Subject area	*Materials Science and Engineering*
More specific subject area	*Solidification of Metallic Alloys*
Type of data	*Table, figures, synchrotron X-ray images, videos and Matlab code*
How data was acquired	*Synchrotron X-ray imaging, high-speed camera, finite element simulation*
Data format	*Raw and analysed*
Experimental factors	*Ultrasound intensity, acoustic pressure, temperature, fatigue strength and life*
Experimental features	*Solidification of metallic alloys under ultrasound*
Data source location	*School of Engineering & Computer Science, University of Hull, Hull, HU6 7RX, UK*
Data accessibility	*The data are available with this article*

Value of the data

- The videos presented clearly demonstrate the microstructural fragmentation induced by ultrasound treatment in a liquid metal.
- The datasets can be used for comparison with other experimental and theoretical results.
- The data on acoustic pressure can be used to determine the ultrasound induced pressure at any depth from the sonotrode tip.
- The Matlab code can be used for future synchrotron X-ray image processing.

1. Data

Table 1 shows the measured amplitudes of the sonotrode tip from the ultrafast X-ray images when different ultrasound powers were applied; and the resulting ultrasonic intensities. Fig. 1 presents the distribution of acoustic pressure in the Bi-8%Zn liquid metal along the distance below the sonotrode tip. Fig. 2 gives the growth in percentage of solid needle-shaped Zn phase during the solidification process of the Bi-8% Zn alloy without ultrasound under a cooling rate of 0.2 °C/s. Fig. 3 demonstrates the experimental data used to determine the material constants for the Zn alloy at 20, 50 and 100 °C. The Matlab code used to obtain the percentage and speed of the solid particles from synchrotron X-ray images is listed in Appendix A. Synchrotron X-ray images in supporting the evidences and arguments presented in Figs. 4–6 and 8 in [1] were processed into videos. Video 1 shows the ultrasonic bubble implosion and shock wave; Video 2 presents the bubble pulsating on a liquid-solid (L-S) interface; Video 3 gives the fragmentation of a needle-shaped Zn particle by an oscillating bubble; Videos 4–6 demonstrate the break-up of the L-S interface by acoustic flow under different ultrasonic intensities.

Supplementary material related to this article can be found online at http://dx.doi.org/10.1016/j.dib.2018.01.110.

Table 1
The measured amplitude of the sonotrode tip under different applied ultrasonic powers. The ultrasonic intensity was calculated using Eq. (1).

Ultrasound power (W)	Amplitude (μm)	Ultrasonic intensity (W/mm^2)
20	30.12	276
40	42.67	553
60	55.22	926
80	65.26	1294
100	77.81	1839

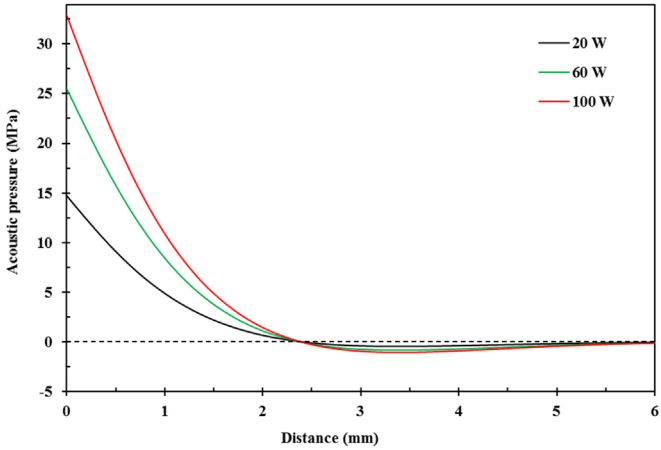

Fig. 1. Distribution of the acoustic pressure along the distance below the sonotrode tip under different powers calculated by using Eq. (2).

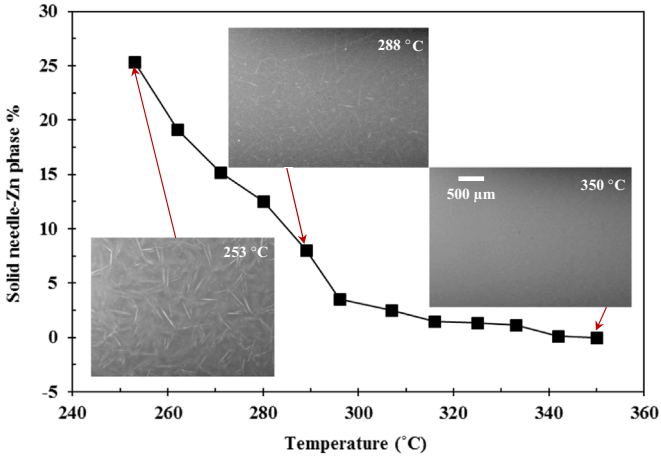

Fig. 2. Growth of the solid Zn phase in percentage during the solidification of the Bi-8% Zn alloy under a cooling rate of 0.2 °C/s. Insets show the real-time X-ray images captured at Beamline I12 using 30 fps.

2. Experimental design, materials and methods

Ultrafast Synchrotron X-ray imaging experiments were carried out to study the effects of ultrasound on the fragmentation of metallic phases during the solidification process as detailed in [1]. A Bi-8%Zn alloy was used because of its low melting temperature and sufficient X-ray contrast between the matrix and the primary Zn phases. A Hielscher UP100H ultrasound processor with a MS2 sonotrode was adopted to introduce ultrasound into the melt. As supplementary to the full research paper [1], this article provides further experimental and simulation data as listed below.

2.1. Ultrasonic intensity

To measure the actual vibration amplitudes of the sonotrode tip, the same ultrasound processor as in [1] was used, with the Ø2 mm sonotrode tip submerged in a distilled water tank (50 × 50 × 50 mm). Ultrasound was applied for 1 s, and a Phantom™ V7.3 high speed camera was used to

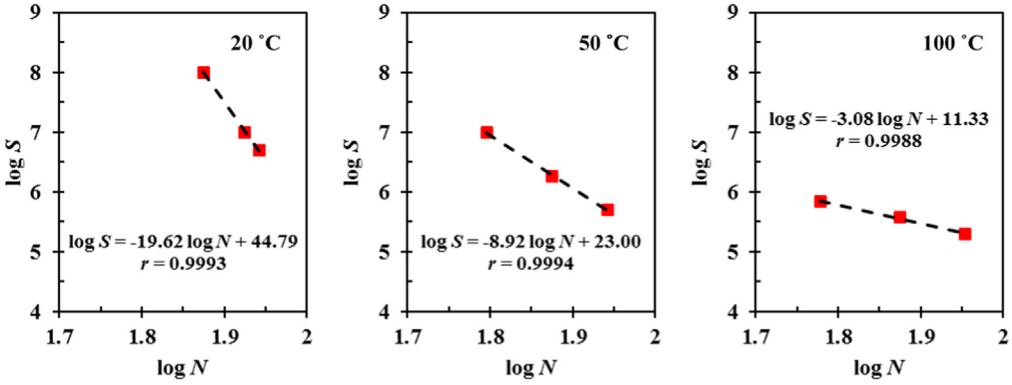

Fig. 3. Experimental data extracted to determine the material constants for the Zn alloy at 20, 50 and 100 °C.

capture the images at 11,000 frame per second (fps) with a spatial resolution of 4.43 μm/pixel. Then, the real vibration amplitudes of the sonotrode tip can be measured from a set of images by using the FIJI [2] software, and the resulting data are listed in Table 1. Therefore, the corresponding ultrasonic intensity, I, can be calculated as below [3]:

$$I = \frac{1}{2}\rho C(A_0\omega)^2 \tag{1}$$

where, ρ is the density of the melt; C is the sound speed in the liquid media; A_0 is the amplitude of the cyclic pressure wave; $\omega = 2\pi f$ is the angular frequency with f being the frequency of the sound wave.

2.2. Acoustic pressure

The alternating acoustic pressure field generated from the ultrasonic waves in a liquid medium attenuates exponentially along the distance below the sonotrode tip [4]. The acoustic pressure, P_a, at a certain depth follows the Helmoholtz equation [5]:

$$\frac{(\omega/C)^2}{\rho}P_a + \nabla\left(\frac{1}{\rho}\nabla P_a\right) = 0 \tag{2}$$

Eq. (2) can be solved by using the finite element-based software COMSOL Multiphysics as detailed in [6]. Fig. 1 presents the distribution of acoustic pressure in the Bi-8%Zn liquid metal along the distance below the sonotrode tip under the ultrasonic power of 20 W, 60 W and 100 W.

2.3. Solidification of the Bi-8%Zn alloy

Solidification of the Bi-8%Zn alloy without ultrasound was monitored by using the synchrotron X-ray imaging at Beamline I-12, Diamond Light Source (DLS), UK. Fig. 2 shows the growth of the solid needle-shaped Zn phase during the solidification process, the insets are the real-time X-ray images captured at 30 fps.

2.4. Fatigue analysis of Zn phases

Experimental data for a commercial Zn-4% Al alloy as reported by Sawalha [7] were used to predict the fatigue behavior of Zn under 270 °C. The fatigue strength, S, and fatigue life, N, of alloys can be calculated by using the Basquin's Law as detailed in [1]. For high-cycle fatigue (with $N > 10^5$ cycles), three data points below 90 MPa were selected at each temperature from [7] to determine the material constants. Fig. 3 shows the linear relationship between (log N) and (log C) at 20, 50 and 100 °C.

2.5. Synchrotron X-ray image processing

The percentage and speed of the detached solid particles were obtained by analyzing the X-ray images using a Matlab script [8]. The code is provided in Appendix A.

Acknowledgements

The authors would like to acknowledge the financial support from the UK Engineering and Physical Sciences Research Council (Grant No. EP/L019884/1, EP/L019825/1, EP/L019965/1), the Royal Society Industry Fellowship (for J. Mi in 2012–2016), and the Hull University & Chinese Scholarship Council (Hull-CSC) PhD Studentship (for D. Tan in 2011–2015). The awards of the synchrotron X-ray beam time (EE8542-1 and NT12131-1) by the Diamond Light Source, UK, and those (GUP 23649 and GUP 26170) by the Advanced Photon Source, Argonne National Laboratory, USA are also gratefully acknowledged. Use of the Advanced Photon Source, an Office of Science User Facility operated for the U.S. Department of Energy (DOE) Office of Science by Argonne National Laboratory, was supported by the U.S. DOE under Contract No. DE-AC02-06CH11357.

Appendix A. Supporting information

Supplementary data associated with this article can be found in the online version at http://dx.doi.org/10.1016/j.dib.2018.01.110.

Transparency document. Supplementary material

Transparency document associated with this article can be found in the online version at http://dx.doi.org/10.1016/j.dib.2018.01.110.

References

[1] B. Wang, D. Tan, T.L. Lee, J.C. Khong, F. Wang, D. Eskin, T. Connolley, K. Fezzaa, J. Mi, Ultrafast synchrotron X-ray imaging studies of microstructure fragmentation in solidification under ultrasound, Acta Mater. 144 (2018) 505–515.
[2] J. Schindelin, I. Arganda-Carreras, E. Frise, V. Kaynig, M. Longair, T. Pietzsch, S. Preibisch, C. Rueden, S. Saalfeld, B. Schmid, J. Tinevez, D.J. White, V. Hartenstein, K. Eliceiri, P. Tomancak, A. Cardona, Fiji - an open-source platform for biological-image analysis, Nat. Methods 9 (7) (2012) 676–682.
[3] G.I. Eskin, D.G. Eskin, Ultrasonic Treatment of Light Alloy Melts, second ed., CRC Press, Boca Raton, 2015.
[4] S. Majumdar, P.S. Kumar, A. Pandit, Effect of liquid-phase properties on ultrasound intensity and cavitational activity, Ultrason. Sonochem. 5 (1998) 113–118.
[5] J. Mi, D. Tan, T.L. Lee, in situ synchrotron X-ray study of ultrasound cavitation and its effect on solidification microstructures, Metall. Mater. Trans. B 46 (2015) 1615–1619.
[6] D. Shu, B. Sun, J. Mi, P.S. Grant, A high-speed imaging and modeling study of dendrite fragmentation caused by ultrasonic cavitation, Metall. Mater. Trans. A 43 (2012) 3755–3766.
[7] K. Sawalha, The fatigue properties of pressure diecast zinc-aluminium based alloys, PhD Thesis, Aston University, United Kingdom, 1991.
[8] D. Tan, T.L. Lee, J.C. Khong, T. Connolley, K. Fezzaa, J. Mi, High-speed synchrotron X-ray imaging studies of the ultrasound shockwave and enhanced flow during metal solidification processes, Metall. Mater. Trans. A 46 (2015) 2851–2861.